

# Opinion formation models on a gradient

Michael T. Gastner,<sup>1,2,3</sup> Nikolitsa Markou,<sup>4</sup> Gunnar Pruessner,<sup>2</sup> and Moez Draief<sup>4</sup>

<sup>1</sup>*Department of Engineering Mathematics, University of Bristol,  
Merchant Venturers Building, Woodland Road, Bristol BS8 1UB, UK*

<sup>2</sup>*Department of Mathematics, Imperial College London,  
South Kensington Campus, London SW7 2AZ, UK*

<sup>3</sup>*Institute of Technical Physics and Materials Science, Research Centre for Natural Sciences,  
Hungarian Academy of Sciences, P.O. Box 49, H-1525 Budapest, Hungary*

<sup>4</sup>*Department of Electrical and Electronic Engineering,  
Imperial College London, South Kensington Campus, London SW7 2AZ, UK*

Statistical physicists have become interested in models of collective social behavior such as opinion formation, where individuals change their inherently preferred opinion if their friends disagree. Real preferences often depend on regional cultural differences, which we model here as a spatial gradient  $g$  in the initial opinion. The gradient does not only add reality to the model. It can also reveal that opinion clusters in two dimensions are typically in the standard (i.e., independent) percolation universality class, thus settling a recent controversy about a non-consensus model. However, we also present a model where the width of the transition between opinions scales  $\propto g^{-1/4}$ , not  $\propto g^{-4/7}$  as in independent percolation, and the cluster size distribution is consistent with first-order percolation.

## I. INTRODUCTION

Disagreement between neighbors costs energy, in human societies as well as in ferromagnetic spin interactions. Because of this similarity, statistical physicists have recently shown great interest in models of opinion formation (e.g. [1–6], see [7, 8] for literature reviews). Individual actors in a population are regarded as nodes in a network and their opinions represent political affiliations, religions or consumer choices (Microsoft Windows<sup>TM</sup> vs. UN\*X, Blu-ray<sup>TM</sup> vs. HD-DVD, etc.). The nodes influence each other’s opinions along the edges in the network according to rules specific to the model in question. Rules that allow a critical mass of like-minded peers to persuade a disagreeing individual have recently found support in behavioral experiments [9]. The resulting opinion dynamics has been linked to election outcomes [10, 11] and innovation diffusion [12, 13], suggesting lessons for political campaigns [14] and advertisement [15].

Many opinion formation models embedded in two-dimensional space have only one stable solution: a complete consensus [3, 5, 16]. In reality, however, perfect agreement is rare [17] – at least one small village of indomitable Gauls always holds out against the Romans. Some models thus allow clusters of a minority opinion to persist even if entirely surrounded by the opposite opinion [18, 19]. In this case, percolation theory provides the tools to analyze the geometry of the minority clusters [19, 20]. However, the results have been controversial [21, 22] because the interactions generate complex correlations that can obscure the familiar scaling laws of uncorrelated percolation. In this article we tackle the open question: can opinion dynamics fundamentally alter percolation properties such as the clusters’ fractal dimensions or the cluster size distribution? We show that in many cases we retrieve the scaling laws of uncorrelated percolation. Moreover, we also give one example where a slight change of the dynamic rules leads to a radically

different scaling behavior.

## II. METHODS

We focus on models where the nodes are placed on a square lattice with edges linking them to their four nearest neighbors. Each node holds one of two possible opinions: “black” or “white”. Initially, the probability to be black is independent at all sites and given by

$$p(x) = gx + p_c, \quad x \in [-p_c/g, (1 - p_c)/g], \quad (1)$$

where  $x$  is the node’s horizontal position and  $g \in \mathbb{R}^+$  a constant gradient. (We set the intercept  $p_c$  equal to the percolation threshold for later convenience.) Thus, nodes on the far left and far right of the lattice are likely to start with opposite opinions. Some previous spatial models have included heterogeneous agents [23–25], but no gradient. In contrast, election results in various countries exhibit clear, smooth gradients, especially between progressive urban and conservative rural areas [26–28]. Our model resembles such a “culture war” fought on a gradient.

A gradient model allows us to analyze, in a single simulation, clusters for a whole interval of  $p$  rather than a single fixed value. On the left of Fig. 1(a)-(c), the black clusters form small isolated islands, whereas on the right a single large black cluster spans from top to bottom [30]. This percolation transition can be characterized by the hull of the spanning cluster [31], defined as the following left-turning walk [29, 32]. We start the walk at a site with minimal  $x$ -coordinate in the black spanning cluster and face towards the right (Fig. 1d). First we attempt to turn to the neighbor on our left, but step in this direction only if we reach a black site. Otherwise, we try to move forward, then to the right, and finally backward until we have discovered the first black neighbor. If we iterate this procedure and apply periodic boundary conditions

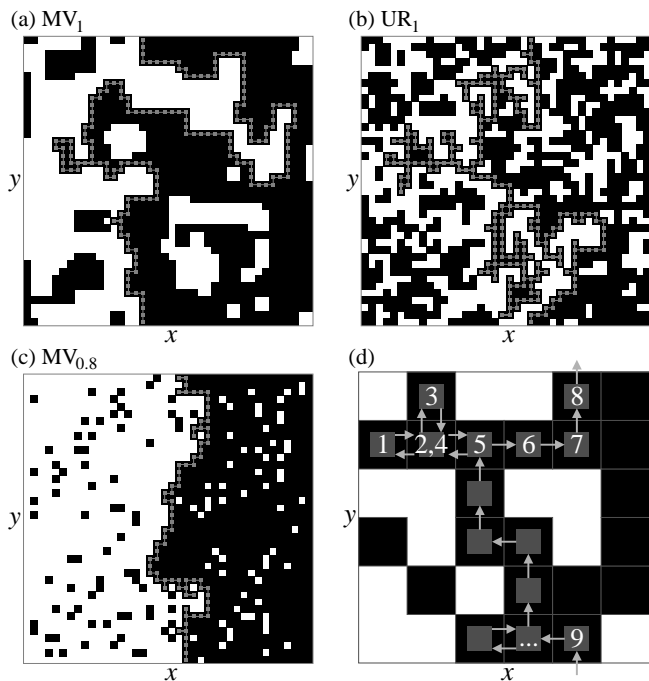


FIG. 1: **Opinion distributions and percolation hull.** We show typical steady-state opinion distributions for  $g = 5 \times 10^{-3}$  and (a)  $MV_1$ , (b)  $UR_1$ , (c)  $MV_{0.8}$ . The two opposing opinions are shown as black and white squares. The sites marked by gray squares form the spanning cluster's hull. (d) Illustration how the hull can be parameterized by a left-turning walk [29].

in the  $y$ -direction, the hull has visited the entire front of the spanning cluster when it returns to the starting position.

We construct the hull in the steady state of the opinion formation models defined by one of the following local rules.

- Majority vote (MV): the node follows the majority opinion of its four neighbors. If both opinions are equally represented, no opinion change occurs.
- Unanimity rule (UR): the node changes its current opinion if and only if all of its neighbors hold the opposite opinion [33].
- Independent percolation (IP): the node keeps its current opinion irrespective of the surrounding opinions.

When a node is updated, it follows the local rule with probability  $q$ . Otherwise it independently chooses a random opinion according to Eq. 1. All nodes simultaneously update their opinion at each time step. For a fixed value of  $q$ , we abbreviate the models by  $MV_q$  or  $UR_q$ , respectively. We do not need a subscript  $q$  for IP because, regardless of the value of  $q$ , any snapshot of the lattice looks statistically alike.

### III. RESULTS AND DISCUSSION

#### A. Steady-state hull width and length

If  $q = 1$ , the dynamics is deterministic and the only source of randomness lies in the initial assignment of opinions. In this special case,  $MV_1$  is identical to the non-consensus opinion model of Ref. [19], where it was already noted that a small fraction of the nodes – in our simulations 1.2% on average at  $p_c = 0.50643(1)$  – keeps switching opinions with period 2. When all other nodes have stopped changing opinions, we will consider  $MV_1$  to have reached its steady state. The convergence is quick: a non-periodic node freezes after a mean of only 0.8 time steps. In  $UR_1$ , oscillatory opinions can occur only if the initial opinions form a perfect checkerboard pattern. Because the gradient pins the left (right) edge to be entirely white (black), a checkerboard pattern is impossible. Hence, every node reaches a stationary opinion, on average after just 0.06 updates at  $p_c = 0.549199(5)$ . For IP, percolation occurs, as in zero-gradient percolation, at  $p_c = 0.59274(1)$  [34].

If  $q < 1$ , the opinions in  $MV_q$  and  $UR_q$  never freeze, but, after a transient, the stochastic time series of black occupancy in any column  $x$  becomes stationary. All measurements for  $q < 1$  presented here were made at  $q = 0.8$  in this steady state. A visual comparison between Fig. 1(a)-(c) suggests a qualitative difference between  $MV_1$  and  $UR_1$  on the one hand and  $MV_{0.8}$  on the other hand. In the latter case, the spanning cluster appears significantly more compact and the hull, which is centred at  $p_c = 0.5000(4)$ , much straighter. So, counterintuitively, the stochastic dynamics of  $MV_{0.8}$  anneals rather than roughens the surface compared to  $MV_1$  and  $UR_1$ .

We can quantify this observation by computing the hull's width  $w$  and length  $l$ . If the hull consists of the walk  $(x_1, y_1), \dots, (x_l, y_l)$ , we define

$$w = \sqrt{\frac{\sum_i x_i^2}{l} - \left(\frac{\sum_i x_i}{l}\right)^2}. \quad (2)$$

As Fig. 2 shows, the width and length scale for all models as power laws  $w \propto g^{-a}$  and  $l \propto g^{-b}$  in the limit  $g \rightarrow 0^+$ . With only one exception among all investigated cases, the results are consistent with  $a = 4/7$  and  $b = 3/7$ , the exact exponents of uncorrelated gradient percolation [35]. We also retrieve the correlation length critical exponent  $\nu$  of standard percolation via the formula  $\nu = a/(a-1) = (1-b)/b = 4/3$  [30]. The notable exception is  $MV_{0.8}$  with  $a = 1/4$  and  $b = 0$ . In uncorrelated percolation,  $a \neq 4/7$  can arise only if the probability to be black increases nonlinearly at the percolation threshold [36]. However, in that case the ratio  $b/a$  must still equal  $3/4$  which is not true for  $MV_{0.8}$  so that we must look elsewhere for an explanation.

We will briefly summarize why  $a$  equals  $1/4$  for  $MV_q$  if  $q$  is close to, but not equal to 1. For details we re-

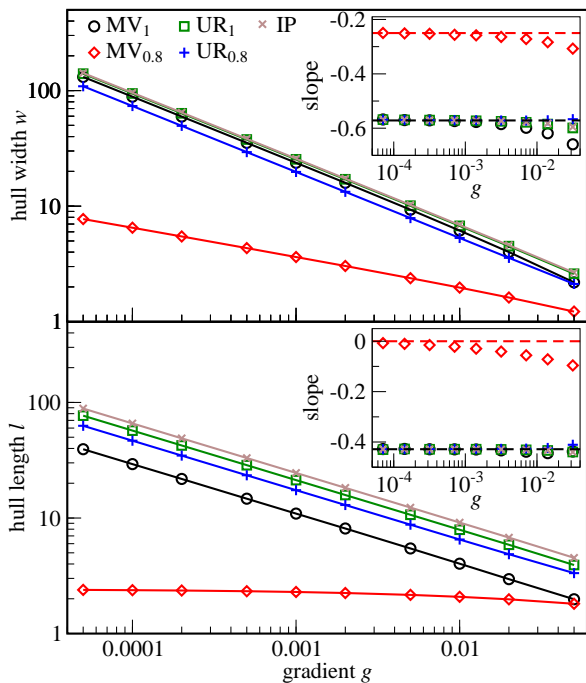


FIG. 2: **Mean hull width and length as a function of the gradient.** Insets: slope in doubly-logarithmic scales (i.e.  $d\log(w)/d\log(g)$  in upper,  $d\log(l)/d\log(g)$  in lower panel). Dashed lines indicate the limiting slopes for  $g \rightarrow 0^+$ :  $-4/7$  and  $-1/4$  in the upper,  $-3/7$  and  $0$  in the lower panel. Error bars are smaller than the symbol sizes.

fer to the online Supporting Information. We make two approximations. (1) The hull can be treated as a single-valued function of  $y$  so that we can parameterize the hull at time  $t$  as a function  $h(t, y)$ . (2) In  $MV_{0.8}$ , as opposed to  $UR_q$  and IP, we observe only few isolated minority nodes, which motivates a “solid-on-solid” approximation: we neglect that there is a small number of black (white) sites to the left (right) of  $h(t, y)$ . With the notation  $r = 1 - q$ , the only transition probabilities for  $h(t, y)$  up to terms of order  $O(r^2)$  are (see Supporting Information)

$$\Pr[h \rightarrow h - 1 + K_y] = r \left[ \frac{1}{2} + g \left( h - \frac{1}{2} + K_y \right) \right], \quad (3)$$

$$\Pr[h \rightarrow h + K_y] = 1 + r(g - 1), \quad (4)$$

$$\Pr[h \rightarrow h + 1 + K_y] = r \left[ \frac{1}{2} - g \left( h + \frac{1}{2} + K_y \right) \right], \quad (5)$$

where  $K_y = +1$  if  $h(t, y)$  is a strict local minimum in  $y$ ,  $K_y = -1$  for a maximum, and  $K_y = 0$  otherwise. In the continuum limit [37], the leading terms in the evolution of the hull are (see Supporting Information)

$$\frac{\partial h}{\partial t} = D \frac{\partial^2 h}{\partial y^2} - Egh + F\eta(t, y), \quad (6)$$

where  $D, E, F$  are independent of  $g$  and  $\eta$  is white noise with mean zero and covariance  $\langle \eta(t, y)\eta(t', y') \rangle =$

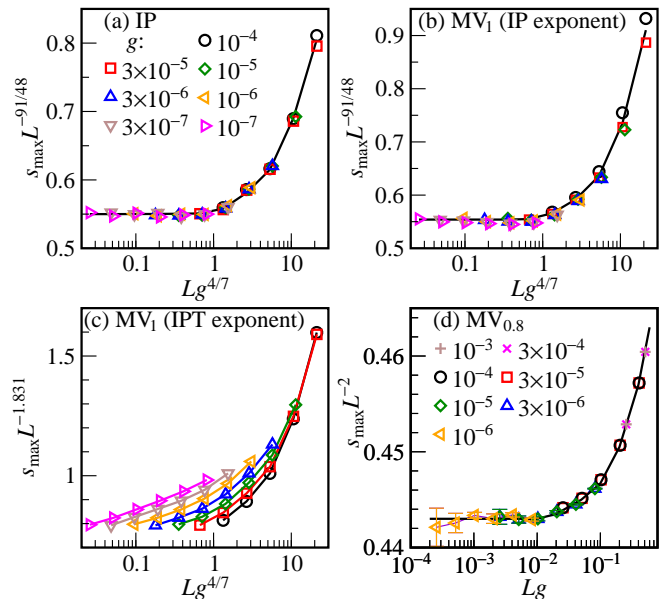


FIG. 3: **Fractal dimensions.** For the correct exponents  $d_f$  and  $c$ ,  $s_{\max}L^{-d_f}$  as a function of  $Lg^c$  should collapse on a single curve with slope zero for  $Lg^c \rightarrow 0$ . For (a) IP and (b)  $MV_1$ ,  $d_f = 91/48$  is the same as the fractal dimension of standard percolation. (c) Replacing  $d_f$  with the value 1.831 of invasion percolation with trapping (IPT) does not produce a data collapse. (d) For the largest  $MV_{0.8}$  cluster, we obtain a data collapse if  $d_f = 2$ .

$\delta(t - t')\delta(y - y')$ . Equation 6 is the Edwards-Wilkinson equation [38] with an Ornstein-Uhlenbeck restoring force [39, 40] and can be integrated (see Supporting Information) to obtain the continuum limit of Eq. 2,

$$w^2 = \lim_{t \rightarrow \infty} \langle \overline{h(t)^2} - \overline{h(t)}^2 \rangle = \frac{F^2}{4\sqrt{DEg}}, \quad (7)$$

where the angle brackets denote the ensemble average and the overlines symbolize spatial averages. Thus, we obtain  $w \propto g^{-1/4}$  consistent with the numerical results for  $MV_{0.8}$ . Although we have here derived the scaling law only for the MV model, numerical evidence suggests that  $a = 1/4$  is valid for a broader class of gradient models. In Ref. [41], a numerical fit for a spatial birth-death process on a gradient also yields  $a = 0.26(1)$ .

## B. Cluster sizes

The scaling laws for  $w$  and  $l$  signal that  $MV_{0.8}$  is not in the same universality class as IP. In Ref. [19] it is claimed that  $MV_1$  is in yet another class, namely invasion percolation with trapping (IPT). Although  $w$  scales identically in IP and IPT [42], we now demonstrate how the gradient method can still show unequivocally that  $MV_1$  belongs to the IP class after all, thus supporting the arguments of Ref. [21]. We calculate the size  $s_{\max}$  of the largest

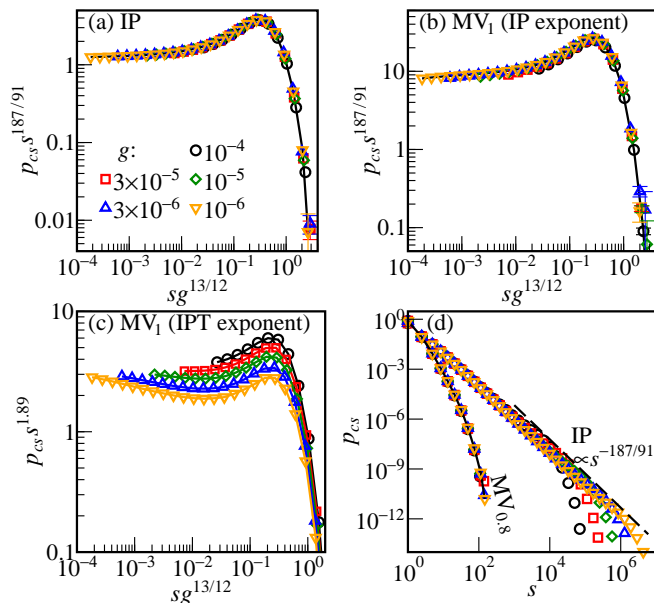


FIG. 4: **Cluster size distributions.** (a) The rescaled distribution  $p_{cs}s^\tau$  for IP collapses if plotted versus  $sg^{1/[\sigma(\nu+1)]}$ , where the critical exponents  $\nu$ ,  $\sigma$ ,  $\tau$  are those of standard percolation. For  $MV_1$  the data collapse is much better (b) for the IP exponent  $\tau = 187/91$  than (c) for the IPT exponent  $\tau = 1.89$ . (d) The  $MV_{0.8}$  distribution does not follow the same asymptotic power law as IP.

cluster in a lattice whose linear size is  $L$  in both  $x$ - and  $y$ -direction. We center the  $x$ -axis at  $p_c$  so that the initial probability to be black in Eq. 1 is limited by  $\pm \frac{1}{2}gL + p_c$  on the right (left) edge. As a function of  $L$  and  $g$ ,  $s_{\max}$  is expected to satisfy the ansatz

$$s_{\max} = L^{d_f} f_{s_{\max}}(L/\xi(g)). \quad (8)$$

Here  $d_f$  is the fractal dimension of the cluster at  $p_c$ ,  $\xi(g)$  is the characteristic length scale for changes in the cluster density, and the scaling function  $f_{s_{\max}}(z)$  approaches a constant for  $z \rightarrow 0^+$ . The fractal dimensions differ between the two universality classes in question:  $d_f = 91/48 \approx 1.896$  for IP and  $d_f = 1.831(3)$  for IPT [43]. Furthermore,  $\xi(g)$  in IP scales linearly with  $w \propto g^{-4/7}$  [30]. Thus, according to Eq. 8, a plot of  $s_{\max}L^{-91/48}$  versus  $Lg^{4/7}$  collapses the IP data for different  $L$  and  $g$  on a single curve that asymptotically approaches a constant for small  $Lg^{4/7}$  (Fig. 3a). For  $MV_1$ , we obtain a data collapse with the same IP exponents (Fig. 3b). By contrast, if we assume  $d_f = 1.831$ , there is neither a collapse nor do the individual curves approach a constant for  $Lg^{4/7} \rightarrow 0^+$  (Fig. 3c), hence ruling out that  $MV_1$  is in the same universality class as IPT [51]. However, the collapse of  $MV_{0.8}$  with  $d_f = 2$  and  $\xi(g) \propto g^{-1}$  in Fig. 3(d) corroborates that opinion dynamics can lead to percolation outside the IP universality class.

The cluster size distribution provides further support for this classification. We count all non-spanning clusters

with at least one site in the stripe  $|x| < w$  and compute the fraction  $p_{cs}(s)$  of clusters of size  $s$ . In IP [41]

$$p_{cs}(s) = s^{-\tau} f_{cs}\left(sg^{1/[\sigma(\nu+1)]}\right), \quad (9)$$

where the critical exponents are  $\tau = 187/91 \approx 2.055$ ,  $\sigma = 36/91$ ,  $\nu = 4/3$  [44], and  $f_{cs}(z) \rightarrow \text{const.}$  for  $z \rightarrow 0^+$  (Fig. 4a). Reference [19] hypothesizes that in  $MV_1$  the exponent  $\tau$  is replaced by 1.89(1), the corresponding value for the pore size distribution in IPT. However, Fig. 4(b) and (c) show that, while the data collapse is excellent for  $\tau = 187/91$ , it is poor for the alternative value 1.89. In summary,  $MV_1$  and IP share the following critical exponents: the hull width and length exponents  $a$ ,  $b$  and consequently  $\nu = 4/3$ ; the fractal dimension  $d_f$  and thus  $\beta = \nu(2 - d_f)$ ; furthermore  $\tau$  and  $\sigma$ . This list is clear evidence that  $MV_1$  is in the IP universality class. As shown in the Supporting Information, we reach the same conclusion for  $UR_1$  and  $UR_{0.8}$ .

The situation is different in  $MV_{0.8}$  where the cluster size distribution appears to drop more sharply with a cutoff that varies much less with the gradient. We want to assess the lack of scaling quantitatively and distinguish it from a power law with large exponent  $\tau$  and little dependence of the upper cutoff on  $g$ . Moment ratios  $s_c^{(n)} = \langle s^{n+1} \rangle / \langle s^n \rangle$  are asymptotically proportional to the upper cutoff, provided  $n > \tau - 1$ . If the transition is continuous, then  $s_c^{(n)}$  scales asymptotically as a power of  $g$ . This power law can be detected more easily than the asymptotic scaling regime  $p_{cs} \propto s^{-\tau}$  [45].

We plot the moment ratios of IP,  $UR_1$ ,  $MV_1$ ,  $UR_{0.8}$  and  $MV_{0.8}$  for  $n = 2, 3, 4$  in Fig. 5. Except  $MV_{0.8}$ , all of these cases are in excellent agreement with the prediction of Eq. 9,  $s_c^{(n)} \propto g^{-1/[\sigma(\nu+1)]}$ , where  $\sigma = 36/91$  and  $\nu = 4/3$  are the critical exponents of IP [44]. The cutoff  $s_c^{(n)}$  in  $MV_{0.8}$ , by contrast, does not diverge as a power law for  $g \rightarrow 0^+$ . Instead  $s_c^{(n)}$  appears to reach an asymptotic value for all  $n$ . Such a behavior is typical of a first-order transition. Based on these data, we can firmly rule out that  $\tau$  in  $MV_{0.8}$  has the IP value  $187/91 \approx 2.055$ . We add the caveat that, for sufficiently large  $n$ ,  $s_c^{(n)}$  may scale as a power of  $g$  after all. However, the data imply  $\tau > 5$ , an unusually large value compared to IP, directed percolation ( $\tau = 2.112$ ) [46] and Achlioptas percolation ( $\tau = 2.04762$ ) [47].

#### IV. CONCLUSION

“Explosive” percolation has become a much discussed topic in statistical physics after Achlioptas et al. [48] conjectured that certain network growth models can lead to a first-order phase transition. The key idea is to add bonds iteratively to an initially empty network in such a way that the emergence of a spanning cluster is delayed for as long as possible. Although the particular algorithm

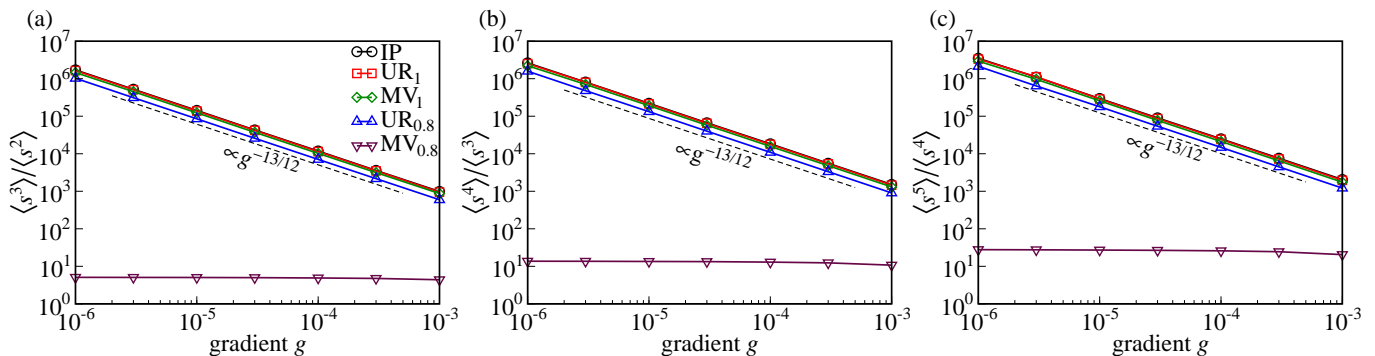


FIG. 5: **Cluster size moment ratios.** The moment ratios  $\langle s^{n+1} \rangle / \langle s^n \rangle$  of the cluster size distributions for (a)  $n = 2$ , (b)  $n = 3$ , (c)  $n = 4$ . The ratios for UR<sub>1</sub>, MV<sub>1</sub>, and UR<sub>0.8</sub> scale in the same manner as in IP, namely  $\langle s^{n+1} \rangle / \langle s^n \rangle \propto g^{13/12}$ . By contrast, the moment ratios for MV<sub>0.8</sub> appear to reach an asymptotic limit for  $g \rightarrow 0^+$ .

of Ref. [48] is now known to generate a continuous transition after all [47, 49], modifications of the original idea indeed appear to produce first-order percolation [50].

Our work highlights a different possible path towards explosive percolation where edges are added or deleted depending on local information about the state of the neighbors rather than global information about cluster sizes. We have chosen a population dynamic model with two stable stationary solutions, where one state is above and the other below the percolation threshold. In MV<sub>0.8</sub> at  $p = 0.5$ , there are stable states with either a black or white majority. Without a gradient, there is hysteresis if one tries to move from one majority to the other by tuning  $p$ . By introducing a gradient, the two phases are forced to collide because the left boundary must be completely white and the right boundary black. We observe that the gradient stabilizes and sharpens the front compared to IP. The birth-death model of Ref. [41] already suggested the possibility of first-order transitions in gradient models. We leave it to future research to

analytically confirm the first-order nature of the MV<sub>0.8</sub> transition. It would also be insightful to investigate more complex network topologies that are based on real social interactions rather than a regular square lattice. We emphasize that, in the light of previous work on explosive percolation, only analytic results can fully clarify the order of any percolation transition. However, we can conclude with certainty that, although none of the opinion models we have investigated is consistent with IPT, MV<sub>0.8</sub> is an example of a dynamic rule that leads to percolation outside the IP universality class.

## V. ACKNOWLEDGMENTS

We gratefully acknowledge support by Imperial College London and the European Commission (project number FP7-PEOPLE-2012-IEF 6-456412013).

- 
- [1] M. J. de Oliveira, J. Stat. Phys. **66**, 273 (1992).
  - [2] K. Sznajd-Weron and J. Sznajd, Int. J. Mod. Phys. C **11**, 1157 (2000).
  - [3] P. L. Krapivsky and S. Redner, Phys. Rev. Lett. **90**, 238701 (2003).
  - [4] S. Galam, Europhys. Lett. **70**, 705 (2005).
  - [5] R. Lambiotte and S. Redner, J. Stat. Mech. **2007**, L10001 (2007).
  - [6] C. Roca, M. Draief, and D. Helbing, in *Social Self-Organization*, edited by D. Helbing (Springer, Berlin, 2012), pp. 169–184.
  - [7] C. Castellano, S. Fortunato, and V. Loreto, Rev. Mod. Phys. **81**, 591 (2009).
  - [8] D. Stauffer, J. Stat. Phys. **151**, 9 (2013).
  - [9] M. Moussaïd, J. E. Kämmer, P. P. Analytis, and H. Neth, PLoS One **8**, e78433 (2013).
  - [10] A. T. Bernardes, D. Stauffer, and J. Kertész, Eur. Phys. J. B **25**, 123 (2002).
  - [11] M. C. González, A. O. Sousa, and H. J. Herrmann, Int. J. Mod. Phys. C **15**, 45 (2004).
  - [12] H. Amini, M. Draief, and M. Lelarge, in *Network Control and Optimization*, edited by E. Altman and A. Chaintreau (Springer, Berlin, 2009), pp. 17–25.
  - [13] A. C. R. Martins, C. de B. Pereira, and R. Vicente, Physica A **388**, 3225 (2009).
  - [14] T. M. Gradowski and R. A. Kosiński, Int. J. Mod. Phys. C **17**, 1327 (2006).
  - [15] D. J. Watts and P. S. Dodds, J. Consum. Res. **34**, 441 (2007).
  - [16] T. M. Liggett, *Stochastic Interacting Systems: Contact, Voter and Exclusion Processes* (Springer, Berlin, 1999), 335 p.
  - [17] P. A. Klinkner, The Forum **2**, 2 (2004).
  - [18] D. Stauffer, J. Math. Sociol. **28**, 25 (2004).
  - [19] J. Shao, S. Havlin, and H. E. Stanley, Phys. Rev. Lett. **103**, 018701 (2009).

- [20] F. Camia, C. M. Newman, and V. Sidoravicius, *Commun. Math. Phys.* **246**, 311 (2004).
- [21] A. Sattari, M. Paczuski, and P. Grassberger, *Phys. Rev. Lett.* **109**, 079801 (2012).
- [22] J. Shao, S. Havlin, and H. E. Stanley, *Phys. Rev. Lett.* **109**, 079802 (2012).
- [23] D. Stauffer and J. S. Sá Martins, *Physica A* **334**, 558 (2004).
- [24] D. Centola, R. Willer, and M. Macy, *Am. J. Sociol.* **110**, 1009 (2005).
- [25] M. Mobilia, A. Petersen, and S. Redner, *J. Stat. Mech.* **2007**, P08029 (2007).
- [26] F. Cutler and R. W. Jenkins, in *Canada: The State of the Federation 2001*, edited by H. Lazar and H. Telford (McGill-Queen's University Press, Montreal, 2002), pp. 367–392.
- [27] R. S. Clem and M. J. Chodakiewicz, *Eurasian Geogr. Econ.* **45**, 475 (2004).
- [28] R. Lang, T. Sanchez, and A. Berube, in *Red, Blue, and Purple America: The Future of Election Demographics*, edited by R. Teixeira (Brookings Institution Press, Washington, 2008), pp. 25–49.
- [29] T. Grossman and A. Aharony, *J. Phys. A: Math. Gen* **19**, L745 (1986).
- [30] B. Sapoval, M. Rosso, and J. F. Gouyet, *J. Physique Lett.* **46**, L149 (1985).
- [31] R. F. Voss, *J. Phys. A: Math. Gen.* **17**, L373 (1984).
- [32] M. T. Gastner, B. Oborny, D. K. Zimmermann, and G. Pruessner, *Am. Nat.* **174**, E23 (2009).
- [33] R. Lambiotte, S. Thurner, and R. Hanel, *Phys. Rev. E* **76**, 046101 (2007).
- [34] M. E. J. Newman and R. M. Ziff, *Phys. Rev. Lett* **85**, 4104 (2000).
- [35] P. Nolin, *Ann. Probab.* **36**, 1748 (2008).
- [36] M. T. Gastner and B. Oborny, *New J. Phys.* **14**, 103019 (2012).
- [37] D. D. Vvedensky, *Phys. Rev. E* **67**, 025102(R) (2003).
- [38] S. F. Edwards and D. R. Wilkinson, *Proc. R. Soc. Lond. A* **381**, 17 (1982).
- [39] G. E. Uhlenbeck and L. S. Ornstein, *Phys. Rev.* **36**, 823 (1930).
- [40] N. G. Van Kampen, *Stochastic Processes in Physics and Chemistry* (Elsevier, Amsterdam, 1992), 480 p.
- [41] M. T. Gastner, B. Oborny, A. B. Ryabov, and B. Blasius, *Phys. Rev. Lett.* **106**, 128103 (2011).
- [42] A. Birovljev, L. Furuberg, J. Feder, T. Jøssang, K. J. Måløy, and A. Aharony, *Phys. Rev. Lett.* **67**, 584 (1991).
- [43] S. Schwarzer, S. Havlin, and A. Bunde, *Phys. Rev. E* **59**, 3262 (1999).
- [44] D. Stauffer and A. Aharony, *Introduction to percolation theory* (Taylor & Francis, London, 1991), 2nd ed., 192 p.
- [45] K. Christensen, N. Farid, G. Pruessner, and M. Stapleton, *Eur. Phys. J. B* **62**, 331 (2008).
- [46] D. Dhar and M. Barma, *J. Phys. C: Solid State Phys.* **14**, L1 (1981).
- [47] R. A. da Costa, S. N. Dorogovtsev, A. V. Goltsev, and J. F. F. Mendes, *Phys. Rev. Lett.* **105**, 255701 (2010).
- [48] D. Achlioptas, R. M. D'Souza, and J. Spencer, *Science* **323**, 1453 (2009).
- [49] O. Riordan and L. Warnke, *Science* **333**, 322 (2011).
- [50] Y. S. Cho, S. Hwang, H. J. Herrmann, and B. Kahng, *Science* **339**, 1185 (2013).
- [51] Changing the exponent  $4/7$  on  $g$  leads to a lateral shift of the data in Fig. 3(c), but we found no value yielding a convincing data collapse. Moreover, it cannot overcome the problem that the hypothetical scaling function  $f_{s_{\max}}(z)$  would not become constant for  $z \rightarrow 0^+$ .